ISSN 0965-545X, Polymer Science, Ser. A, 2011, Vol. 53, No. 4, pp. 303–310. © Pleiades Publishing, Ltd., 2011.
Original Russian Text © D.A. Panchuk, Zh.K. Sadakbaeva, D.V. Bagrov, A.V. Bol'shakova, L.M. Yarysheva, I.B. Meshkov, A.M. Muzafarov, A.L. Volynskii, N.F. Bakeev, 2011, published in Vysokomolekulyarnye Soedineniya, Ser. A, 2011, Vol. 53, No. 4, pp. 539–546.

Estimating the Strain–Strength Characteristics of Nanothick Nonmetallic Coatings Deposited onto Poly(ethylene terephthalate) Films[1]

D. A. Panchuk[a], Zh. K. Sadakbaeva[a], D. V. Bagrov[b], A. V. Bol'shakova[a], L. M. Yarysheva[a], I. B. Meshkov[c], A. M. Muzafarov[c], A. L. Volynskii[a], and N. F. Bakeev[a]

[a] *Faculty of Chemistry, Moscow State University, Moscow, 119991 Russia*
[b] *Faculty of Physics, Moscow State University, Moscow, 119991 Russia*
[c] *Institute of Synthetic Polymer Materials, Russian Academy of Sciences, Profsoyuznaya ul. 70, Moscow, 117393 Russia*
e-mail: pandaa85@rambler.ru

Received April 8, 2010;
Revised Manuscript Received November 18, 2010

Abstract—The features of surface structuring during tensile drawing of PET films with deposited nanothick coatings are studied. In contrast to our earlier studies, this investigation is focused on the study of nonmetallic coatings (carbon deposited by vacuum sputtering and modified silica deposited via evaporation from the solution). In both cases, the tensile drawing of the supporting polymer is accompanied by the fragmentation of deposited coatings on PET films and by the development of regular surface patterns. The above features (i) demonstrate the general character of the phenomena occurring during tensile drawing of the polymer films and (ii) have allowed the first quantitative estimation of the strain–strength characteristics of the deposited coatings (modified silica gel) in nanoscale layers.

DOI: 10.1134/S0965545X11040079

INTRODUCTION

Studying the physicomechanical characteristics of films featuring thin solid coatings with nanoscale thicknesses has evident academic and applied importance. These materials can be used as oxygen-resistant materials; flexible mirrors; and conducting, sensing, and magnetic materials. Their volumes of production are gradually increasing. For example, PET films coated with silicone dioxide have proved themselves as excellent oxygen-resistant materials in the food and pharmaceutical industries [1]. In addition, metallized polymer films are widely used in microelectronics [2]. Evidently, on the one hand, the practical use of the above materials requires knowledge of the mechanisms of fracture of the deposited coatings. On the other hand, this study is crucial for the analysis of the fundamental characteristics of a substance scaled down to nanometric dimensions. The worldwide nanotechnological boom demands the acquisition of new knowledge on the correlation between the nanostructure and characteristics of such materials. However, despite the vital importance of any information about the characteristics of substances on the nanoscale, problems of their estimation are far from being solved. In particular, information on the strain–strength characteristics of solids with dimensions ranging from several to tens of nanometers is scarce, and this deficit of knowledge is the direct consequence of evident experimental difficulties in performing tests on such tiny materials. Therefore, advances in the development of new methods for the characterization of the above materials are very important.

With consideration for the above reasoning, the results of our recent studies on the estimation of the strain–strength characteristics of nanometric coatings deposited onto polymer films seem very promising. These results are based on the study of the structural parameters of the fracture of coated polymer films during the tensile drawing of the supporting polymer. Remember that tensile drawing of polymer films with thin solid coatings is accompanied by spontaneous development of a regular pattern on their surface and by the fragmentation of the coating. These phenomena have a general character and are observed in all "rigid coating on a soft substratum" systems, independently of their scale. In all cases when such a system is developed (either by deposition of thin coatings onto polymers [3, 4] or in some natural processes [5]), its deformation is accompanied by spontaneous development of a regular surface pattern. These structural features of "rigid coating on a soft substratum" systems control the above phenomenon, whose mechanism was described in detail in [6–9]. Note some of the fundamental structural features of "rigid coating on a soft

[1] This work was supported by the State Program for the Support of Leading Scientific Schools (NSh 4371.2010.3) and State Contract no. 02.740.11.0143.

substratum" systems: The thickness of the coating should be negligibly small in comparison to the thickness of the supporting material, and the elastic modulus of the coating should be at least an order of magnitude higher than the elastic modulus of the supporting material.

The proposed approach to estimating the mechanical characteristics of nanothick coatings is based on the earlier developed [6–9] correlation between the parameters of the surface pattern formed owing to the deformation of polymer films with coatings and the characteristics of the materials of the coating and the support. Estimation of the strain–strength characteristics of nanoscale solids by the methods described in [10, 11] were performed for coatings based on noble metals deposited via ionic plasma sputtering. At the same time, according to [12], the mode of deposition of gold (ionic plasma deposition or thermal sputtering) onto a PET-based support has a certain effect on the structure and, thus, on the characteristics of the deposited coatings. Note that the above formulated conditions for the development of "rigid coating on a soft substratum" systems are not limited by the nature of a deposited coating, a circumstance that allows the conclusion that the proposed approach [10, 11] can be successfully used for the analysis of the strain–strength characteristics of all coatings, including coatings based on nonmetallic compounds.

In this context, the goals of this study are (i) to investigate the effect of the nature of a nanothick coating and the mode of its deposition onto the polymer support on the character of surface structuring induced by the deformation of the PET-based polymer support and (ii) to estimate the strain—strength characteristics of coatings.

EXPERIMENTAL

In this study, we investigated the commercial films based on amorphous unoriented PET with a thickness of 100 μm. The samples were cut as dumbbell-shaped specimens with a gage size of 6 mm × 20 mm. The surfaces of the above films were decorated with layers of a trimethylsilyl-group-modified molecular silica sol prepared according to the following scheme [13].

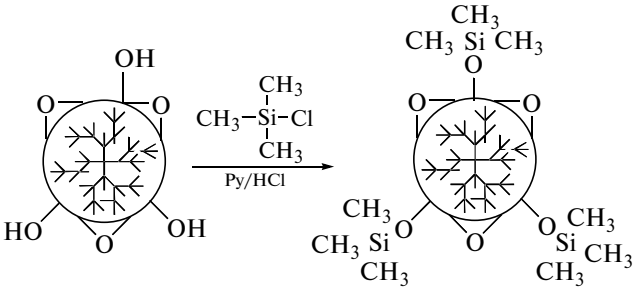

This product, called silica sol, is a soluble modification of modified silica [14]. When silica sol is deposited onto the support and the solvent is evaporated, an amorphous coating based on modified silica is formed. Hereinafter, this coating is referred to as modified silica or *m*-silica. The polymer films coated with an *m*-silica layer were prepared via immersion of the PET film in a 3% solution of silica sol in heptane. The thickness of the deposited coating was controlled by the number of repeated immersions of the film in the solution; this parameter was estimated from the weight gain of the films before and after immersion in the silica sol solution. The solvent was removed from the films by air drying until a constant weight was attained.

Thin carbon layers were deposited onto the film surface via thermal vacuum sputtering. The thickness of the carbon coatings was estimated according to the following procedure. A test polymer film and a reference cover glass were placed in a Jee 4B vacuum sputtering unit (Japan Electron Optics Lab Co., Tokyo). After deposition of the carbon coating via thermal evaporation in vacuum, the carbon-coated glass plate was scratched with a wooden stick and the depth of the scratch was measured with a Nanoscope-2 atomic force microscope (Digital Instruments, Santa Barbara, United States) under the regime of contact forces. The profilograms of the AFM images allowed precise estimation of the thickness of the deposited coatings. The structure of the deposited layers was examined via the method of transmission electron microscopy (TEM). The thickness of the supporting polymer was high (~100 μm); hence, for the TEM observations, the test films were sectioned into thin slices with a thickness of ~100 nm by a Reichert–Jung microtome with a diamond knife.

The tensile drawing of the films was performed on an Instron-1122 universal tensile machine at 20 and 90°C. In the mechanical tests, the crosshead speed was 10 mm/min. After stretching at temperatures above the T_g of the polymer, samples fixed in the clamps of the stretching machine were cooled to room temperature and then released.

The structure of the surfaces of the stretched films was examined on a Hitachi S-520 scanning electron microscope, on a LEO 912AB transmission electron microscope equipped with an OMEGA filter, and on a Nanoscope-IIIa atomic force microscope. Numerical values of the average dimensions of the fractured fragments of the deposited coatings and the period of the surface micropattern were estimated from the corresponding electron microscopic images with the use of the program FemtoScan Online [14].

The strength of the deposited coatings was calculated according to the relationship proposed in [10, 11]:

$$\sigma^* = L\sigma_0/3h, \quad (1)$$

where L is the size of the fractured fragment of the deposited coating along the direction of tensile drawing of the supporting polymer, h is the thickness of the deposited coating, σ^* is the strength, and σ_0 is the stress in the support.

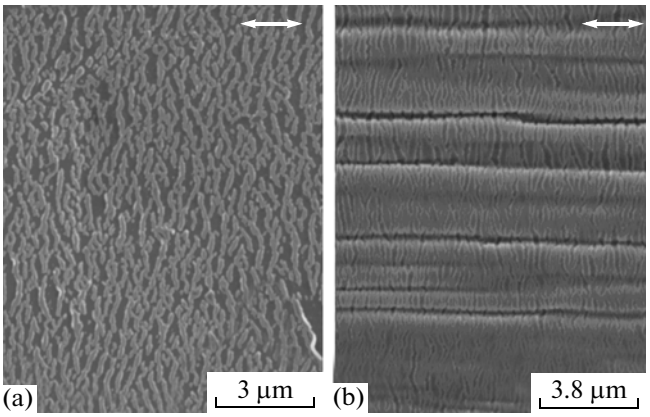

Fig. 1. SEM images of the fracture of modified silica coatings on a PET support after tensile drawing at (a) 20 and (b) 90°C. The coating thicknesses are (a) 77 and (b) 100 nm. The direction of tensile drawing is shown by the arrow.

The tensile strain of the coating was estimated from the following relationship [10, 11]:

$$\varepsilon_{coating} = \frac{L_{coating}}{L_{overall}}\lambda_{polym} - 1 \quad (2)$$

Here, $\varepsilon_{coating}$ is the irreversible (plastic) tensile strain of the coating, $L_{coating}$ is the sum of all lengths of the fractured fragments of the deposited coating along the direction of tensile drawing of the supporting polymer, $L_{overall}$ is the length of the fragment of the sample for which $L_{coating}$ was measured, and λ_{polym} is the tensile strain of the supporting polymer. All details of the calculation procedure have been described in [7–9].

RESULTS AND DISCUSSION

Nanothick Coatings Based on m-Silica

The main results of estimating the strengths of the coatings according to the approach advanced in [6–9] were obtained in our earlier studies for metallic coatings.

According to the objectives of the study, coatings based on *m*-silica were used; the mode of their deposition onto the PET-based films was described in Experimental. Figure 1 shows the SEM images of the fractured surface of the *m*-silica coatings deposited onto the PET-based support after tensile drawing at 20°C (a coating thickness of 77 nm) and 90°C (a coating thickness of 100 nm). As follows from Fig. 1, the tensile drawing of the PET films with the *m*-silica coating is accompanied by the fracture of the coating and entails, as in the case of tensile drawing of films coated with metallic layers, formation of the fractured fragments located in the direction perpendicular to the axis of the tensile drawing of the polymer. For the rubbery state of the polymer support (the tensile drawing of PET at 90°C), the fragmentation of the coating is aggravated by the development of a surface micropattern in the form of a set of irregular folds located along the direction of tensile drawing of the sample. Note that, because of the tensile drawing of the PET film with the *m*-silica coating (a coating thickness of ~100 nm), the formed surface pattern contains very large folds and smaller fractured fragments of the coating. This fact is the main difference between the behavior of the silica-based coatings and the behavior of the metallic coatings, for which the dimensions of the fractured fragments are comparable to the period of the surface micropattern.

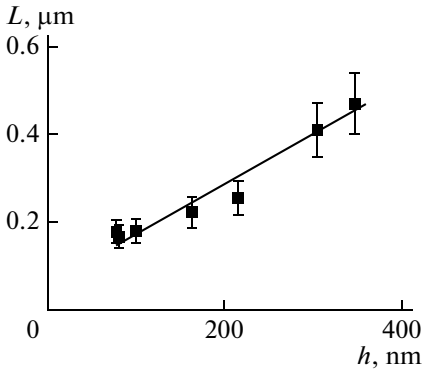

Fig. 2. Average width of the fractured fragments of the silica-based coating plotted against the thickness of the deposited coating at 20°C.

For the *m*-silica-coated PET films with different coating thicknesses, the widths of the fractured fragments on the surface were measured. Figure 2 presents the average width of the fractured fragments of the *m*-silica-based coatings plotted against the thickness of the deposited coating at 20°C. As follows from Fig. 2, similarly to the case of the metallic coatings, with an increase in the coating thickness, the widths of the fractured fragments increase. This outcome reveals the general character of the studied phenomena of fracture of the coating during tensile drawing of the supporting polymer, independently of the nature of the coating.

The results of our calculations according to the proposed approach for the *m*-silica coating are displayed in Fig. 3, where coating strength is plotted coating thickness. With a decrease in the thickness of the deposited coating (below 150 nm), the strength increases. If it is assumed that, at a high thickness, the coating strength corresponds to the coating strength in the bulk, it may be expected that the strength of the modified silica coating is ~20 MPa.

In this context, note that a similar phenomenon was observed for a coating based on silicon oxide (unmodified silica) in [15]. Therefore, it is possible to study the effect of the modification of silica on the mechanical characteristics. In [15], according to the analytical model and the derived equation, the strength and the fracture energy for the initial stage of the process were calculated. In the interval of low

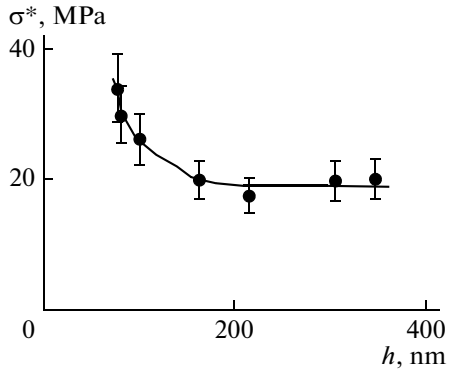

Fig. 3. Strength of the silica-based coating plotted against the thickness of the deposited coating at 20°C.

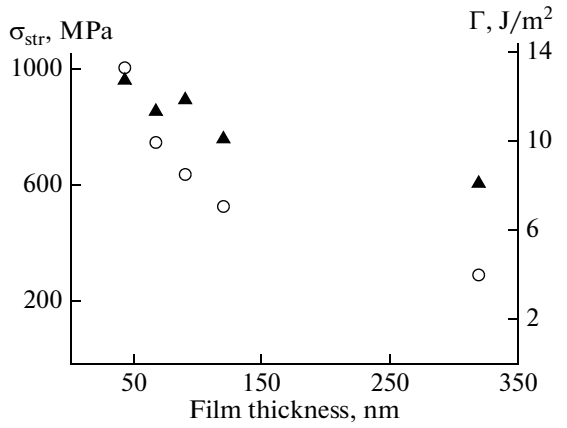

Fig. 4. (Open circles) Calculated strength of the film, σ_{str}, and (closed circles) the energy of fracture, Γ, for the SiO_x-based coating of the PET substrate. The calculations are based on the measurements of the critical applied stress at the initial stages of fracture of the coating.

thicknesses, the above parameters increase. Figure 4 shows the results of our calculations [15].

Similar data typical for the initial stage of fracture of a silicon oxide coating deposited onto a PET support (a tensile strain below 2%) were reported in [16, 17]. The dependence of the cohesive strength and the adhesive strength of an organosilicon coating on film thickness was found. Note that the adhesive strength characterizes the adherence between the coating and the support. This parameter is measured during normal detachment or tangential shear in units of force per area (MPa). The cohesive strength is the mechanical strength of the material provided by molecular cohesion under the influence of attractive forces (forces of intermolecular interaction, hydrogen and chemical bonding) acting between contacting surfaces of two similar bodies. The presented data were obtained also according to theoretical models that relate the characteristics of the fracture of the coating and the characteristics of the coating and the support. The calculated adhesion approaches 75 MPa and does not depend on the coating thickness. The cohesive strength decreases with an increase in coating thickness. Figure 5 shows the results of our calculations: The strength decreases with an increase in the coating thickness. Note that, relative to *m*-silica, the unmodified silica has a higher strength.

Therefore, independently of the nature of the deposited coating (either modified or unmodified silica), the strength characteristics increase in the interval of low thicknesses. Note that, in both cases, we are dealing with an amorphous coating and, nowadays, there is no literature evidence on theoretical predictions of an increase in strength with a decrease in thickness.

In addition to estimation of the coating strength during its fracture, the proposed structural approach makes it possible to calculate another important characteristic of the coating: its plastic or tensile strain. Therefore, we calculated the tensile strain of the *m*-silica coating achieved via the tensile drawing of the supporting polymer.

Figure 6 shows the tensile strain plotted against the thickness of the *m*-silica coating. As follows from Fig. 6, with a decrease in the thickness of the coating, the tensile strain of the silica coating increases.

The coating is ductile and its elongation at break is lower than that of the supporting polymer; hence, the coating can be studied in terms of the structural–mechanical approach. Quantitative estimates of the mechanical characteristics of *m*-silica were obtained. In contrast to the conventional unmodified silica, this coating is not brittle, but actually is composed of a polymer with typical polymer mechanical characteristics (low strength and high elongation at break).

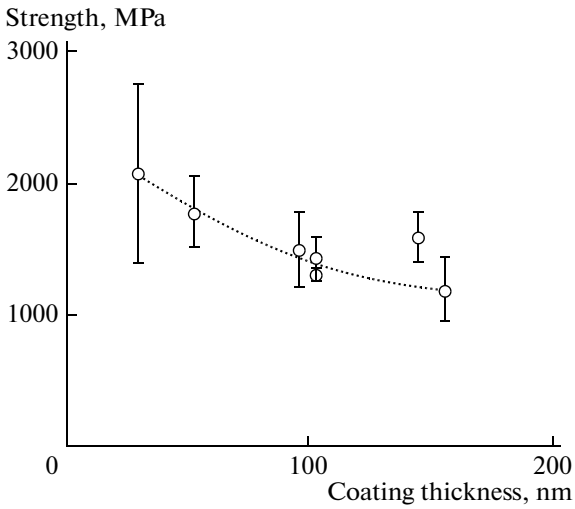

Fig. 5. Cohesive strength of the silica-based coating plotted against its thickness.

Nanothick Coatings Based on Amorphous Carbon

As was mentioned above, in this study, PET films coated with a carbon layer were investigated also. Carbon was selected because, in contrast to the fracture of metals capable of marked plastic strains (up to 50%) [10, 11], its fracture is not accompanied by any marked strains. In addition, carbon was selected because the mode of its deposition (the thermal method) is different from that of the metallic coating. According to [12], the mode of deposition can control the structure of the resultant material. In addition, analysis of the nonmetallic coating deposited via some alternative method is necessary to verify the universal character of the proposed approach for estimating the strain–strength characteristics of nanothick layers deposited onto polymer supports.

Analysis of the characteristics of carbon films is important as well from the viewpoint of diverse areas of their practical application. Thin carbon layers are promising materials for diverse biomedical applications, such as tissue regeneration, controlled drug delivery, surface coatings for bone implants, and improved immune protection. In addition, ultrathin carbon films are used for analytical purposes [18]. According to [19], the presence of the carbon-containing structure has a favorable effect on biocompatibility between polymers and living cells. Carbon layers can possess different structures and can be deposited via different methods; moreover, they can show different characteristics. According to the literature data, thermal sputtering makes it possible to produce thin layers of amorphous carbon and their characteristics depend on the sputtering conditions, in particular, temperature [19].

Let us now consider the consequences of the tensile drawing of the polymer film with the carbon coating. Figure 7a shows the microscopic image of the surface layer of the PET film with the carbon coating after tensile drawing by 50% above the glass-transition temperature of the supporting polymer. The coating breaks down, and this breakdown is accompanied by formation of fractured fragments that appear as ribbons oriented perpendicularly to the direction of tensile drawing. In addition, a regular surface pattern related to the side contraction of the polymer sample during tensile drawing forms. Figures 7b and 7c present microscopic images and AFM images (the corresponding cross section and three-dimensional reconstruction) of the carbon-coated PET films after tensile drawing at room temperature. As follows from these data, because of the tensile drawing of the sample at 20°C, the coating detaches from the polymer matrix. Note that this peeling occurs owing to the side contraction of the PET film during tensile drawing. (The fragments of the regular surface pattern become detached.) At the same time, the coating undergoes regular fragmentation. This result indicates that adhesion is sufficient for the fragmentation and that the proposed approach can be used for estimating the strength characteristics of the coating.

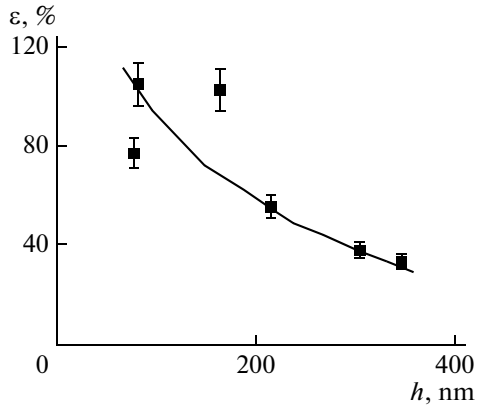

Fig. 6. Ductility of the silica-based coating plotted against thickness of the deposited coating at 20°C.

In this study, the structure of the carbon coating was investigated. To this end, thin sections of PET films with coatings of different thicknesses were examined. Figure 8 shows the typical cross section of a carbon-coated PET sample. The coating is continuous. The integrity and continuity of the coating are confirmed by the fact that the tensile drawing of the supporting polymer is accompanied by fragmentation of the coating and by development of a surface pattern. In particular, according to [20], if the coating is not continuous, the tensile drawing of the coated polymer sample entails no fragmentation and the particles drift away from each other. In other words, the fragmentation of the coating occurs only when the coating is continuous.

Prior to calculating the strength characteristics of the coating, we studied the dependence of the parameters of the structure formed via tensile drawing on the coating thickness. Figure 9 shows the average dimensions of the fractured fragments of the carbon coating plotted against the coating thickness after tensile drawing at 90°C. The widths of fractured fragments was analyzed only when the temperature of tensile drawing exceeded the glass-transition temperature of PET, because, as was mentioned above, the tensile drawing of the sample at room temperature is accompanied by detachment of the coating from the polymer matrix (Figs. 7b, 7c).

Despite a marked scatter in the experimental data, the average size of the fractured fragments increases as the thickness of the carbon-based layer increases. This result agrees with Eq. (1) and justifies its use for estimating the strength of the carbon coating.

Figure 10 presents the carbon-coating strength plotted against the layer thickness. The data were obtained according to Eq. (1). In the interval of low thicknesses (5–15 nm), the tensile strength of the

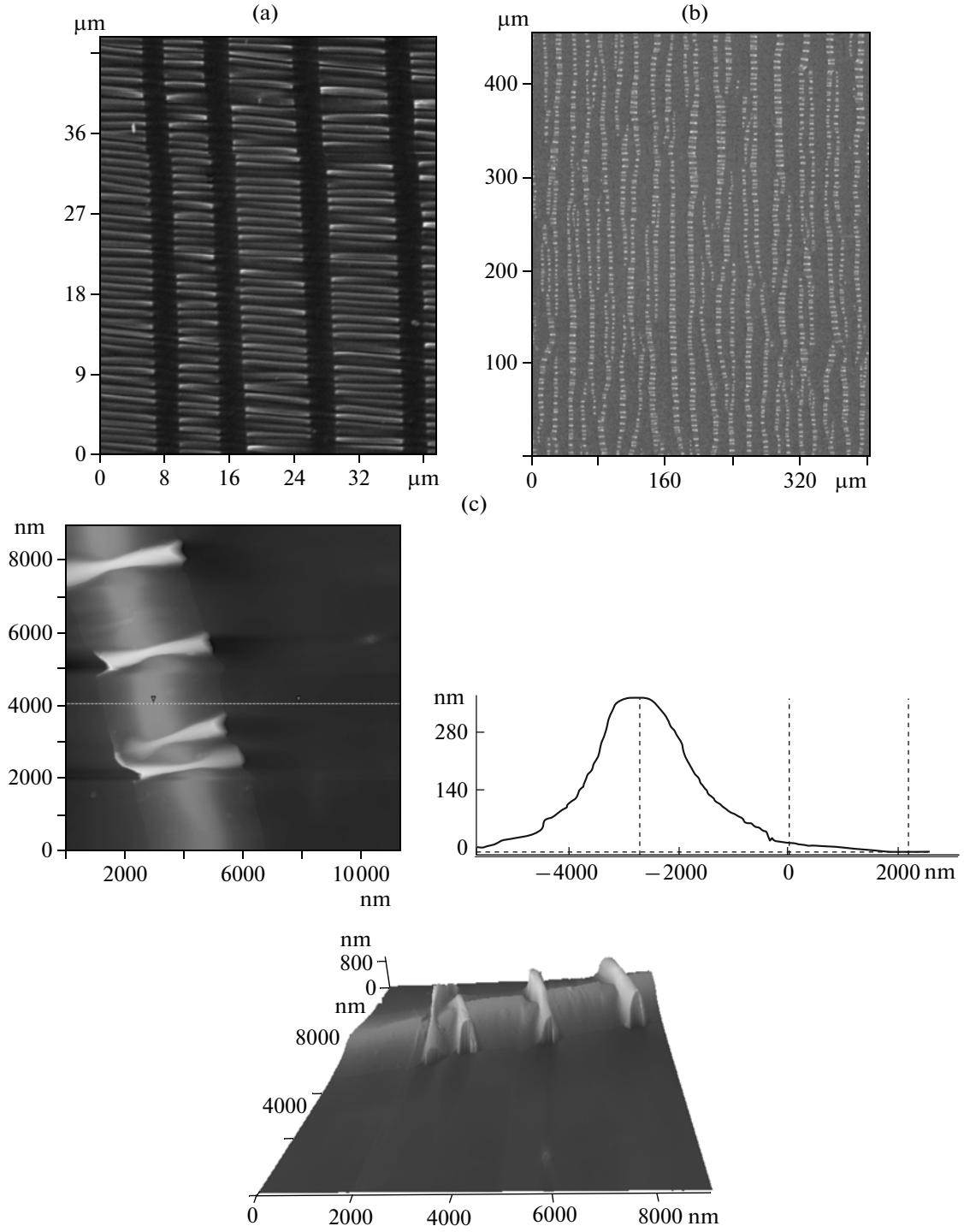

Fig. 7. (a) Micrographs of the PET-based sample with the carbon coating with a thickness of 22 nm after tensile drawing in air by 50% at 90°C; (b) microscopic images of the PET-based samples with carbon coatings with a thickness of 40 nm after tensile drawing in air at 20°C; and (c) the AFM image, the cross section profile, and the three-dimensional reconstruction of an individual fractured fragment.

sample increases. For the layers with a thickness above 20 nm, the coating strength becomes constant.

Amorphous carbon without any admixtures of other components (metals, hydrogen, etc.), as well as amorphous materials with a certain structure (e.g., tetrahedral amorphous carbon [21, 22], amorphous diamondlike carbon [23, 24]), can be obtained either as films deposited onto substrates (e.g., onto silicon,

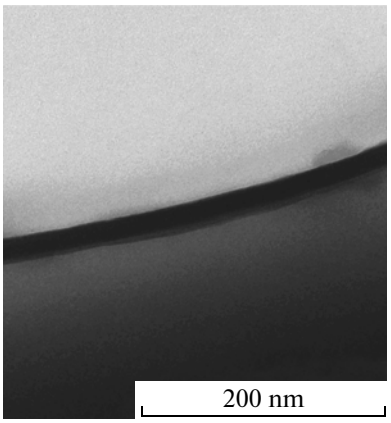

Fig. 8. The TEM image of the 20-nm-thick carbon-based layer deposited onto a PET support by vacuum thermal sputtering.

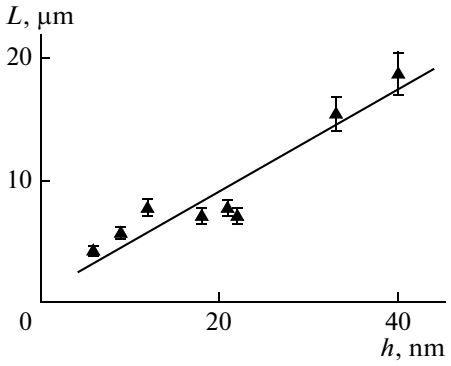

Fig. 9. The width of fractured fragments of carbon-based coatings plotted against the thickness of the coating for the PET support after tensile drawing by 50% at 90°C.

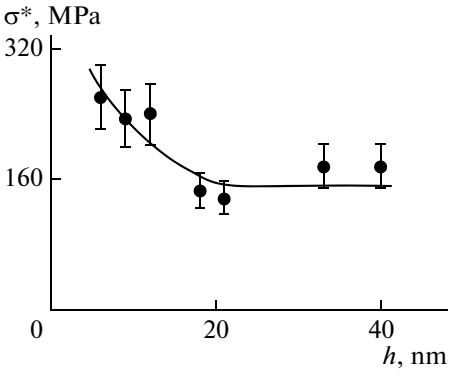

Fig. 10. Strength of the carbon-based coating plotted against thickness of the deposited layer for the PET support after tensile drawing by 50% at 90°C.

polymers) or as nanopowders. Films of amorphous carbon are usually processed via the methods of thermal vacuum deposition from the vapor phase, such as arc discharge, sputtering of particles, pulse laser deposition [19]. The nanopowders based on amorphous carbon are prepared under high pressure from other modifications of carbon, such as graphite [25] and fullerite [26]. There are no detailed and correct literature data on the strength of coatings based on amorphous carbon. An analysis of the mechanical characteristics is primarily reduced to estimation of Young's modulus and the rigidity/hardness of the samples via the method of nanoindentation or computer-aided simulation. Several studies focused on finding the dependence of the above characteristics on the indentation depth corresponding to the penetration of the plunger of a nanoindentor into the sample rather than on the thickness of the deposited coating layer [19, 27, 28]. Therefore, the data presented in the current study are pioneering results on this estimation.

CONCLUSIONS

The general scenario of fragmentation and development of the surface pattern of *m*-silica and carbon coatings on a PET support has been studied. The scenario of the fracture of the coatings is similar to the structuring of metallic coatings deposited onto the polymer support via tensile drawing of the sample. The mechanical characteristics of *m*-silica and carbon coatings in nanothick layers have been estimated according to the microscopic technique of fragmentation. The proposed approach for estimating the mechanical characteristics of solids in nanothick layers has a universal character and may be applied for coatings of diverse natures (polymer or inorganic). Although the causes of the increase in the strength in the interval of low thicknesses of the coating remain vague, both strength and ductility increase, a result that is common for various nanothick coatings deposited onto polymer films.

REFERENCES

1. J. T. Felts, J. Plast. Film Sheet. **9**, 201 (1993).
2. Z. Suo, J. Vlassak, and S. Wagner, *China Particuology 3*, 321 (2005).
3. A. L. Volynskii, I. V. Chernov, and N. F. Bakeev, Dokl. Akad. Nauk **355**, 491 (1997).
4. A. L. Volynskii, S. L. Bazhenov, O. V. Lebedeva, et al., Polymer Science, Ser. A **39**, 1212 (1997) [Vysokomol. Soedin., Ser. A **39**, 1805 (1997)].
5. A. L. Volynskii and S. L. Bazhenov, Eur. Phys. J. E **24**, 317 (2007).
6. A. L. Volynskii, S. L. Bazhenov, and N. F. Bakeev, Ross. Khim. Zh. **42** (3), 57 (1998).
7. A. L. Volynskii, S. L. Bazhenov, O. V. Lebedeva, and N. F. Bakeev, J. Mater. Sci. **35**, 547 (2000).
8. A. L. Volynskii, S. L. Bazhenov, O. V. Lebedeva, et al., J. Appl. Polym. Sci. **72**, 1267 (1999).
9. S. L. Bazhenov, A. L. Volynskii, V. M. Alexandrov, and N. F. Bakeev, J. Polym. Sci., Part B: Polym. Phys. **40**, 10 (2002).

10. A. L. Volynskii, D. A. Panchuk, S. V. Moiseeva, et al., Ross. Nanotekhnol. **3** (1–2), 95 (2008).
11. A. L. Volynskii, S. V. Moiseeva, L. M. Yarysheva, and N. F. Bakeev, Dokl. Akad. Nauk **409**, 64 (2006).
12. V. Svorcik, P. Slepicka, J. Svorcikova, et al., J. Appl. Polym. Sci. **99**, 1698 (2006).
13. N. V. Voronina, I. B. Meshkov, V. D. Myakushev, et al., Ross. Nanotekhnol. **3** (5–6), 77 (2008).
14. A. S. Filonov and I. V. Yaminskii, *Guide of User of Program Software for Control of Scanning Probe Microscope and Image Processing "FemtoScan Online." Version 2.0.5.1* (Tsentr Perspektivnykh Tekhnologii, Moscow, 2004) [in Russian].
15. C. H. Hsueh and M. Yanaka, J. Mater. Sci. **38**, 1809 (2003).
16. Y. Leterrier, J. Andersons, Y. Pitton, and J.-A. Manson, J. Polym. Sci., Part B: Polym. Phys. **35**, 1463 (1997).
17. Y. Leterrier, L. Boogh, J. Andersons, and J.-A. Manson, J. Polym. Sci., Part B: Polym. Phys. **35**, 1449 (1997).
18. V. Svorcik, T. Hubacek, P. Slepicka, et al., Carbon **47**, 1770 (2009).
19. V. Svorcik, O. Kubova, P. Slepicka, et al., J. Mater. Sci., Mater. Med. **17**, 229 (2006).
20. J. S. Trent, I. Palley, and E. Baer, J. Mater. Sci. **18**, 331 (1981).
21. E. Martinez, J. L. Andujar, M. C. Polo, et al., Diamond Relat. Mater. **10**, 145 (2001).
22. D. Lui, G. Benstetter, and E. Lodermeier, Thin Solid Films **436**, 244 (2003).
23. J. Zhu, J. Han, A. Liu, et al., Surf. Coat. Technol. **201**, 6667 (2007).
24. C. E. Bottani, A. Lamperti, L. Nobili, and P. M. Ossi, Thin Solid Films **433**, 149 (2003).
25. A. F. Goncharov, Pis'ma Zh. Eksp. Teor. Fiz. **51**, 368 (1990).
26. V. V. Brazhkin, A. G. Lyapin, Yu. V. Antonov, et al., Pis'ma Zh. Eksp. Teor. Fiz. **62**, 328 (1995).
27. S. Logothetidis, Int. J. Mod. Phys., Nos. 2–3, 113 (2000).
28. S. Logothetidis, C. Charitidis, M. Gioti, et al., Diamond Relat. Mater. **9**, 756 (2000).